Liquids with permanent porosity

Giri, N., Del Pópolo, M. G., Melaugh, G., Greenaway, R. L., Rätzke, K., Koschine, T., Pison, L., Gomes, M. F. C., Cooper, A. I., & James, S. L. (2015). Liquids with permanent porosity. *Nature*, *527*(7577), 216-220. https://doi.org/10.1038/nature16072

Published in:
Nature

Document Version:
Peer reviewed version

Queen's University Belfast - Research Portal:
Link to publication record in Queen's University Belfast Research Portal

Liquids with permanent microporosity

Nicola Giri,[1] Mario Del Pópolo,[2,3] Gavin Melaugh,[2] Rebecca L. Greenaway,[4] Klaus Rätzke,[5] Tönjes Koschine,[5] Margarida F. Costa Gomes,[6] Laure Pison,[6] Andrew I. Cooper[4] and Stuart L. James[1*]

[1] School of Chemistry and Chemical Engineering, Queen's University Belfast, David Keir Building, Stranmillis Road, Belfast, Northern Ireland BT9 5AG, UK. S.James@qub.ac.uk

[2] School of Mathematics and Physics, Queen's University Belfast, University Road, Belfast, Northern Ireland, BT7 1NN.

[3] CONICET & Facultad de Ciencias Exactas y Naturales, Universidad Nacional de Cuyo, Mendoza, Argentina.

[4] University of Liverpool, Department of Chemistry & Centre for Materials Discovery, Crown Street, Liverpool L69 7ZD, UK.

[5] Technische Fakultät der Universität Kiel, Institut für Materialwissenschaft, Materialverbunde, Prof. Dr. F. Faupel Kaiserstr. 2, D-24143 Kiel, Germany.

[6] Institut de Chimie de Clermont-Ferrand, UMR 6296, CNRS, Université Blaise Pascal, 63177 Aubière, France.

Porous solids such as zeolites[1] and metal-organic frameworks[2,3] are useful in molecular separation and in catalysis, but their solid nature can impose limitations. For example, liquid solvents, rather than porous solids, are the most mature technology for post-combustion carbon dioxide capture because liquid circulation systems are more easily retrofitted to existing plants. Solid porous adsorbents offer major benefits, such as lower energy penalties in adsorption–desorption cycles[4], but they are difficult to implement in conventional flow processes. Hence, new materials that combine the properties of fluidity and permanent porosity could offer unique technological advantages. However, permanent porosity is not associated with conventional liquids.[5] Here we report the first free-flowing liquids whose bulk properties are determined by their permanent microporosity. To achieve this, we designed new cage molecules[6,7] that provide a well-defined pore space. These cages are highly soluble in solvents whose molecules are too large to enter the pores. The concentration of unoccupied cages can thus be around 500 times greater than in other molecular solutions that contain cavities[8-10]. As a result, there is a dramatic change in bulk properties, such as an 8-fold increase in the solubility of methane gas. Our results provide the basis to develop a new class of functional porous materials for chemical processes, and we present a one-step, multigram scale-up route for highly soluble 'scrambled' porous cages that is based on commercially available reagents. The unifying design principle for these materials is the avoidance of functional groups that can penetrate into the cage cavities.

The structural rigidity and robustness of solids allows them to contain permanent, uniform cavities of precise size and shape. By contrast, liquids have fluid structures, and any 'porosity' is

limited to poorly-defined and transient intermolecular cavities[11], most of which are smaller than typical molecules. The Scaled Particle Theory[12,13] predicts that the solubility of a solute in a liquid is primarily influenced by the work required to generate the cavities that accommodate the solute. Thus, if high concentrations of permanent, molecule-sized cavities could be created in a liquid, then the solvating and solute-transporting characteristics should be strongly affected[5,14,15]. For example, solutes might become much more soluble because no work would be required to create cavities[12,13]. This effect should be specific to solute molecules of complementary size and shape to the pores, as is common for selective adsorption in porous solids.

We have prepared 'porous liquids' by taking rigid organic cage molecules, each of which defines a molecular pore space, and dissolving them at high concentration in a solvent that is too large to enter the pores (Figure 1). Hence, the pores in the cages remain empty and available to solutes. In our first system, a crown ether, 15-crown-5, was chosen as the solvent because it is a liquid at room temperature and because it consists of large molecules with low surface curvature. Hence, no part of any solvent molecule can fit into the cage pores. Into this solvent were dissolved rigid organic cages. Each cage has a cavity of *ca*. 5 Å diameter at its center that is accessible through four access windows of *ca.* 4 Å in diameter. Structurally similar but much less soluble cages are known to absorb small gas molecules into their pores in the solid state[6,7]. To achieve high solubility in the bulky 15-crown-5 solvent, each cage was functionalized on the outside with six crown ether groups. As a result, we could prepare at room temperature an extremely concentrated liquid phase (44 wt. %) where just 12 solvent molecules are needed to dissolve each cage molecule. More typical solutions of molecules with cavities contain many hundreds or thousands of solvent molecules for each cavity. The liquid flows at room temperature, despite the high concentration of cages. The viscosity of the liquid was 20 to >140 cP in the range 298–

323 K, depending on the cage concentration (Supplementary Figure 10); the viscosity of neat 15-crown-5 is 8.9–22.4 cP over this temperature range. Neat organic cages can also form liquid phases close to room temperature if they have long alkyl chain substituents, but in those cases the chains occupy the cage cavities, thus removing the porosity.[14]

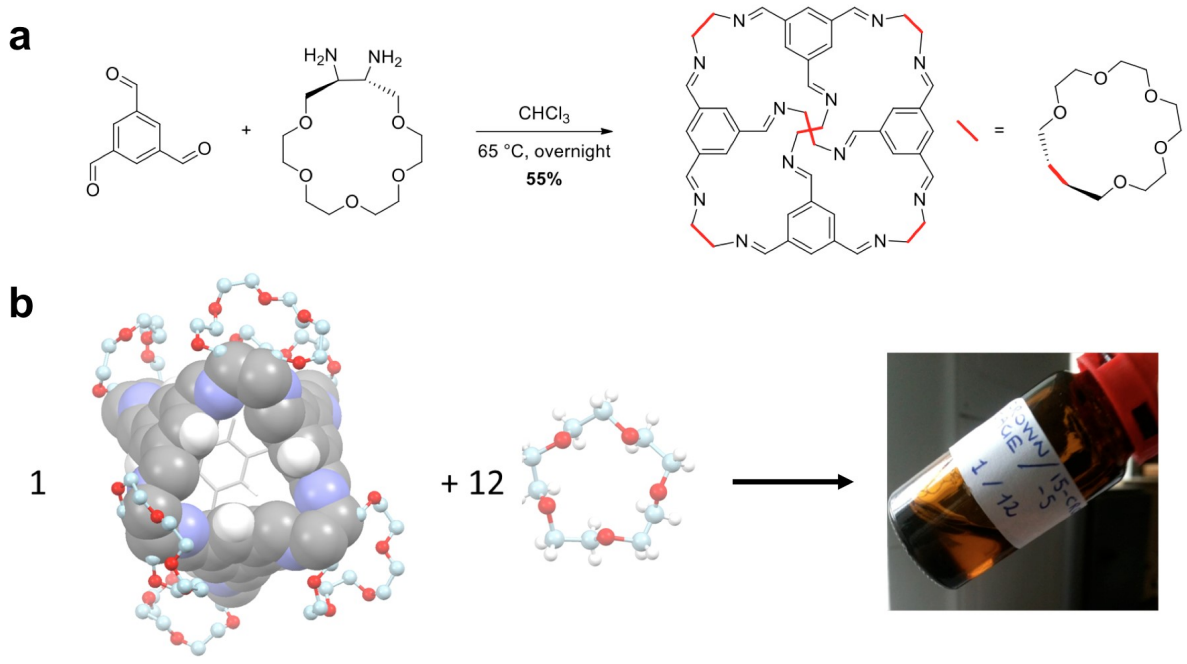

Figure 1. **Preparation of the porous liquid**. **a**, Synthesis of the crown-ether cage. **b**, The highly soluble cage molecule, left, defines the pore space; the 15-crown-5 solvent, middle, provides fluidity but is too large to enter the cage cavities. The concentrated solution flows readily at room temperature, right.

Molecular dynamics (MD) simulations gave detailed insight into the structure of this 'porous liquid'. Over 100 ns simulations, 100 % of the cages remained empty at all times, both at 350 K

and 400 K. Further modelling confirmed that occupation of the cages by the 15-crown-5 solvent molecules, or by the crown ether substituents on the outside of the cages, would incur high free energy costs (full details in the Supplementary Information). In fact, the potential of mean force computed along a reaction coordinate that eventually forces the occupation of the cage by a crown solvent molecule shows no energy minimum when the solvent is inside the cage (Supplementary Figure 14). Therefore, the cages can be concluded to remain empty in the neat porous liquid over longer time scales.

The distribution of cavity sizes, $\rho(R)$, was computed for both the porous liquid, $\rho_{mix}(R)$, and the pure 15-crown-5 solvent, $\rho_{sol}(R)$, at the same temperature and pressure. $\rho(R)$ is the so-called insertion probability, which measures the likelihood that a hard sphere of radius R could be inserted at any arbitrary point within the liquid without overlapping with the van der Waals volume of any atom of the liquid[11]. The snapshot in Figure 2a represents a typical configuration in the MD simulation for the 1:12 mixture at 350 K. The coloured surfaces show the empty cavities both inside (red) and outside (yellow) the cage cores, which are accessible to spherical probes of radius 2.0–2.6 Å. This probe radius range was chosen because it reveals the cavities that are sufficiently large to accommodate methane as a solute molecule. Figure 2a shows that the cage cavities account for most of the large, molecule-sized cavities in the liquid. This can be quantified with respect to the pure 15-crown-5 solvent by calculating the relative porosity of the mixture, defined as $V_{rel}(R) = \rho_{mix}(R)/\rho_{sol}(R)$. A value of $V_{rel}(R)$ greater than one indicates that the fractional free volume accessible to a spherical probe of radius R is larger in the porous liquid than in the pure solvent. As might be expected, the cages have no effect on the concentration of small, sub-molecular cavities in the liquid, and $V_{rel}(R)$ is around 1 for $R < 0.1$ nm (Figure 2b). However, the cages dramatically increase the concentration of molecule-sized cavities with radii

between 0.1–0.25 nm. This effect is particularly strong at 350 K, where $V_{rel}(R)$ approaches 1900 for R = 0.24 nm. $V_{rel}(R)$ is larger at 350 K than at 400 K because more large cavities form transiently in the solvent at higher temperatures due to increased thermal motion. Overall, the fractional void volume in the porous liquid due the cages was estimated as 0.7 % of the total volume. This is small compared to typical pore volumes in porous solids but it can dramatically affect the solubility of solutes in the liquid.

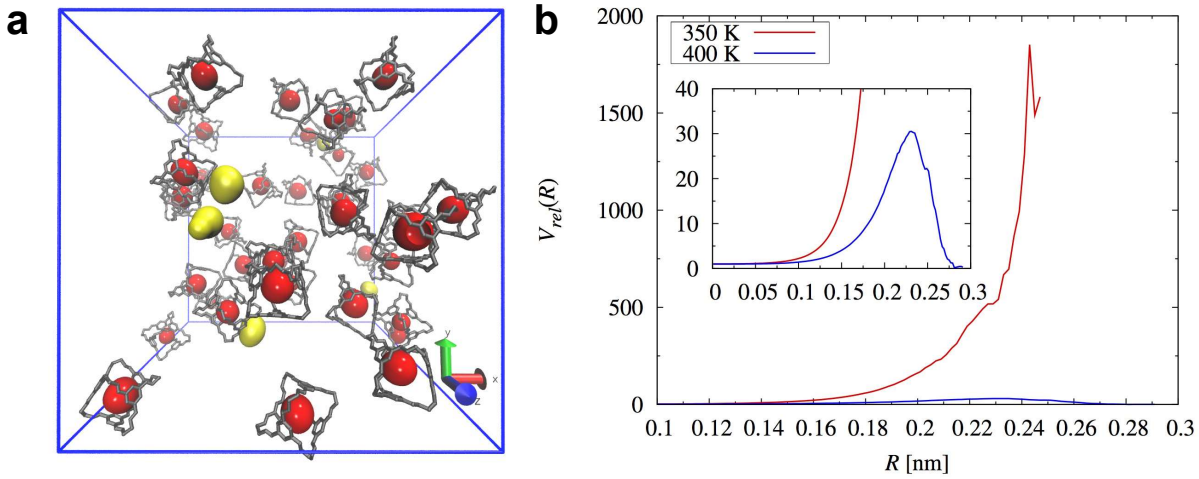

Figure 2. **Molecular simulations for the porous liquid show unoccupied molecular-sized pores. a**, Representative configuration of the porous liquid at 350 K. To highlight the cage cores, all crown ether solvent molecules and crown ether substituents on the cages have been omitted. Red and yellow surfaces indicate empty pores located inside or outside the cages, respectively. **b**, Calculated relative porosity, $V_{rel}(R)$, of the porous liquid at 350 K and 400 K. The inset is an expansion of the 400 K result. At 350 K, the porous liquid has around 1900 times as many methane-sized cavities (probe radius ~0.24 nm) than does the pure solvent.

Positron annihilation lifetime spectroscopy (PALS) experiments were used to investigate whether the cages in the porous liquid were empty. PALS probes the electron density distribution

in materials, in particular the presence of empty pores. In insulating materials, ortho-Positronium (o-Ps) is generated, and its lifetime can be correlated to the average pore diameter in the material by a well-established model[16]. Thus, by comparing the o-Ps lifetimes observed in the pure (solid) cage material, the pure 15-crown-5 solvent, and the porous liquid, we investigated whether the cages in the porous liquid were empty. Several measurements were made on each material to check for reproducibility and to enable separation of the raw data for the porous liquid into constituent components. The o-Ps lifetime of 2.05 +/- 0.1 ns measured for the pure cage at +30 ^{o}C correlates to an average cavity diameter of 0.55 nm, in reasonable agreement with our MD simulations, above. The o-Ps lifetime of 3.00 +/- 0.1 ns for the pure 15-crown-5 solvent at +30 ^{o}C is also in agreement with previous literature[17]. It does not indicate any pre-existing pores in the pure the pure 15-crown-5 solvent, but instead the known phenomenon of o-Ps bubble formation[17]. The o-Ps lifetime measured for the porous liquid at +30 ^{o}C was 2.34 +/- 0.02 ns. If the cages are empty in the porous liquid, then the o-Ps lifetime for the porous liquid should correspond to a combination of the lifetimes measured for the pure cage and the pure 15-crown-5 solvent. To investigate whether the o-Ps lifetime for the porous liquid could be separated into these individual contributions, both free and forced fits were applied to the raw data. Allowing both components to refine freely did not give a satisfactorily clear separation (large error bars were observed, see Supplementary Information). However, a forced fit in which one component was fixed at 3.00 ns, consistent with the anticipated contribution from the pure 15-crown-5 solvent, and in which the other component was allowed to refine freely, did result in satisfactory separation of these two components (see Supplementary Information). The freely refined component had a value of 1.91 +/- 0.08 ns which corresponds well to the lifetime observed for

the pure empty cage (see above). The PALS measurements are thus consistent with the presence of empty cages (*i.e.* pores) in the porous liquid.

Both MD simulations and PALS suggested that the porous liquid might have a dramatically increased capacity to dissolve solutes up to *ca*. 0.5 nm in diameter relative to the pure crown solvent, particularly at lower temperatures (Fig. 2b). Acidic gases, such as carbon dioxide, are absorbed readily by water or by aqueous amines[4]. We therefore focused on methane, the main component of natural gas. Methane, like other important gases such as hydrogen, lacks the Lewis acidity of carbon dioxide and hence cannot be absorbed using liquid amines. The methane solubility in pure 15-crown-5 at 30 °C was found to be 6.7 μmol g^{-1}. By contrast, the solubility of methane in the porous liquid was 52 μmol g^{-1} at 30 °C. This represents, approximately, an 8-fold increase in solubility in the porous liquid compared to the pure solvent. The methane solubility decreased at higher temperatures, both in the porous liquid and in the non-porous solvent, but the solubility was much higher in the porous liquid at all temperatures studied (Figure 3).

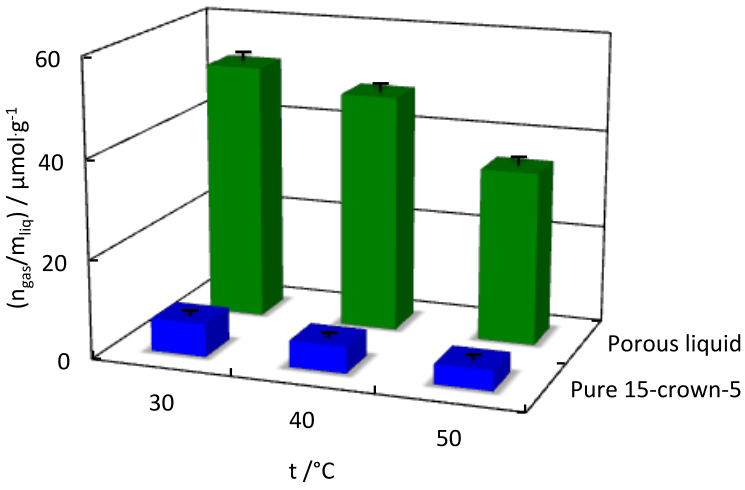

Figure 3. **Methane solubility for the porous liquid (in green) and the non-porous 15-crown-5 solvent (in blue).** The gas is around 8 times more soluble per mass of the porous liquid at

1 atm pressure than per mass of the pure solvent. This corresponds to a 13-fold increase in solubility per mole of porous liquid. The error bars represent the estimated overall uncertainty of the experimental data.

Molecular simulations of solutions of methane in the porous liquid suggested that most methane molecules would be located in the cage cavities, rather than in transient intermolecular cavities (Figure 4; see also Supplementary Information for details). For example, at 350 K and a gas pressure of 1 atm, 70 % of the methane molecules in the liquid were located inside the cages; that is, less than 2.5 Å from a cage centre. These simulations support the methane solubility measurements by predicting that methane should be significantly more soluble in the porous liquid. The enhanced solubility cannot be ascribed to a simple solvating effect of the aromatic cage walls because methane solubility in pure aromatic solvents, such as benzene, is lower than for the porous liquid (26.8 $\mu mol \cdot g^{-1}$ at 25 °C)[18,19]. The methane absorption capacity is remarkably high for a liquid, albeit much lower than many porous solids, such as zeolitic imidazolate frameworks[20].

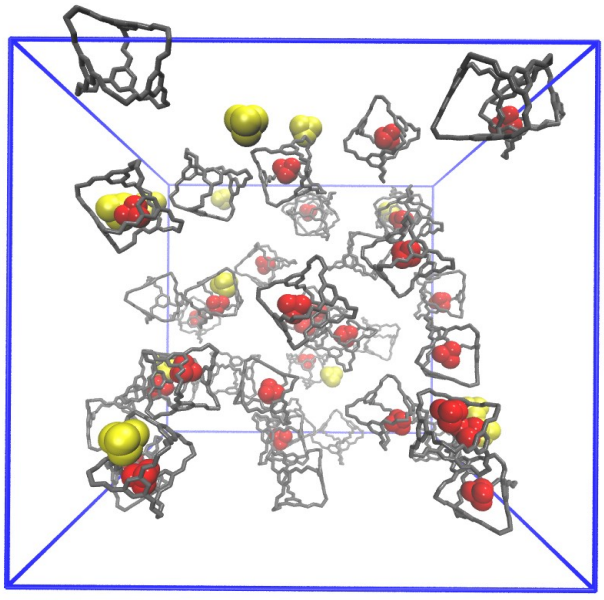

Figure 4. **Molecular simulation of methane solubility in the porous liquid.** Snapshot generated during a Grand Canonical Monte Carlo simulation showing a sample configuration of the 1:12 mixture at 350 K under a methane pressure of 1 atm. Methane molecules are shown in red whenever they lie inside a cage core; that is, less than 2.5 Å from the geometric center of the cage. Methane molecules are shown in yellow when outside of a cage core. Solvent molecules and crown-ether substituents on the cage molecules have been omitted for clarity.

This porous liquid differs fundamentally from porous dispersions of hollow colloidal silica spheres,[21] where the voids in the liquid are much larger than the molecule scale. Solutions of other types of organic cages with smaller internal pores, known as carcerands and cryptophanes, also have pores that are most likely unsolvated because even relatively small solvent molecules are excluded[8-10]. The existence of permanent cavities was not, however, supported by simulations or by PALS measurements, nor was enhanced bulk solubility of gases noted in those studies. This is probably because the solutions were very dilute; for example, based on a 2 mM host solution of a cryptophane in $CDCl_3$, as described in ref. 10, the molar ratio of cage to solvent molecules was 1:6000, compared with the 1:12 solution that we study here. The cryptophane cavity volume in that study[10] was reported to be 81 $Å^3$; if the cryptophane is assumed not to have collapsed, this represents just 0.01 % of the total volume, which is 70 times lower than in our study. The much higher density of cavities in our system demonstrates a previously unexplored way to control the bulk solubility of gases and other solutes in liquids.

While these porous liquids might not compete with porous solids for gas storage, we envisage other applications, such as gas separations, which utilize the high concentration of prefabricated cavities in the liquid. A practical scale up issue is the six-step cage synthesis, which has modest

overall yield (3.1–6.5 %). The viscosity of the crown ether porous liquid is also rather high (20 to >140 cP). We therefore developed an alternative, more scalable route, where a mixture of diamines is used to make a 'scrambled' cage.[22] The resulting mixture of scrambled cage molecules has much higher solubility than similar cages prepared from a single diamine (see table, Fig. 5a) because of increased structural disorder.[23]

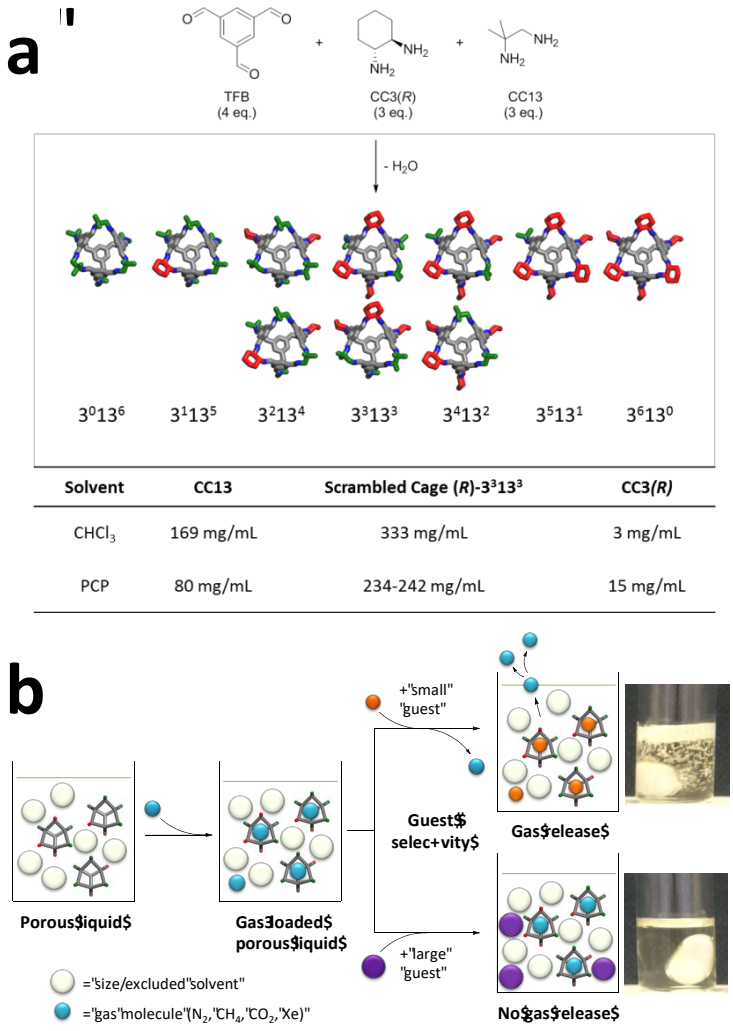

Solvent	CC13	Scrambled Cage (*R*)-3³13³	CC3(*R*)
$CHCl_3$	169 mg/mL	333 mg/mL	3 mg/mL
PCP	80 mg/mL	234-242 mg/mL	15 mg/mL

Figure 5. **One-pot synthesis of 'scrambled' porous liquids with enhanced gas solubility. a**, Mixtures of scrambled cage molecules were prepared in a scalable, one-pot synthesis. These desymmetrized cages are up to 100 times more soluble than cages prepared from single diamines, such as CC3-*R*[6] or CC13.[23] PCP is hexachloropropene, a bulky solvent that is size-

excluded from the scrambled cage cavities. **b**, The scrambled porous liquids show enhanced solubilities for methane and also for other gases such as N_2, CO_2, and xenon (Supplementary Figures 32–35). Again, the scrambled cages contain no functional groups that can penetrate into the cage cavities. To illustrate this principle, addition of a small, interpenetrating guest ($CHCl_3$) liberates xenon gas rapidly from a xenon-saturated porous liquid solution (top photograph; see also Supplementary Video 1). By contrast, addition of a large, size-excluded guest, 1-*t*-butyl-3,5-dimethylbenzene, results in no gas evolution (bottom photograph).

Multi-gram quantities of the scrambled cage are easily prepared from commercially available starting materials via this one-step synthesis (Fig. 5a; 77 % yield). As for the crown-cage, scrambled cages can form concentrated solutions (10 wt. %) in a size-excluded solvent, hexachloropropene (PCP). These solutions were at least ten times less viscous (11.7 cP at 295 K, 0.112 mmol/g cage in PCP) than solutions of the crown-cage porous liquid at comparable cage concentrations, probably because of the lack of bulky crown-ether substituents. The scrambled porous liquids showed much higher methane gas solubilities than the non-porous PCP solvent (51 μmol/g versus 6.7 μmol/g at 293 K), which is similar to the crown-cage porous liquid (Figure 3). Other gases such as nitrogen, carbon dioxide and xenon also showed enhanced solubilities, and the trend in gas solubility matched the calculated Henry's coefficients and isosteric heats of sorption for these gases in *solid* porous cages of this size and geometry[24] (Supplementary Figure 35), again suggesting that gas solubility is dominated by the unoccupied cage cavities. A shift in the ^{1}H NMR signal for methane was observed from -0.24 ppm in neat hexachloropropene to -2.80 ppm in the porous liquid (Supplementary Figure 30). This strong shielding effect ($\Delta\delta$ = -2.56 ppm) supports the presence of methane in the cage cavity on the NMR timescale.[25,26]

As for the crown-cage porous liquids, the increased gas solubility stems from the absence of functional groups that can penetrate the cage cavities. For example, addition of chloroform displaces xenon from a xenon-saturated scrambled porous liquid, whereas addition of a larger, size-excluded guest, 1-*t*-butyl-3,5-dimethylbenzene, does not (Fig. 5b; Supplementary Video 1). This allows dramatic solubility switching to occur with the addition of a remarkably small amount of a cosolvent trigger. For example, 10.05 mL of xenon is released by the addition of just 0.046 mL of $CHCl_3$ to 5.9 g of the porous liquid.

METHODS SUMMARY

Synthesis of the porous crown ether cage. The cage was prepared in six steps. The details for the 5-step synthesis of the crown-ether diamine, (15*S*,16*S*)-1,4,7,10,13-pentaoxacycloheptadecane-15,16-diamine, are given in the Supplementary Information. Reaction of this diamine (6 equiv.) with 1,3,5-triformylbenzene (4 equiv.) in chloroform at 60 °C gave the desired imine cage in a one-pot [4+6] cycloimination reaction (Figure 1a).[6,7] Mpt decomposes >180 °C; **IR** (ν_{max}/cm^{-1}) 2858, 1649, 1598, 1445, 1352, 1298, 1250, 1111, 978, 943, 882; ^{1}H NMR (500 MHz, $CDCl_3$) δ_H 8.12 (12H, s), 7.92 (12H, s), 4.03 (12 H, d, J = 7.0 Hz), 3.75–3.58 (120 H, m); ^{13}C NMR (126 MHz, $CDCl_3$) δ_C 161.06, 136.56, 130.20, 73.25, 72.68, 71.70, 71.09, 70.87, 70.60; HRMS (ES+) calc. for $C_{108}H_{156}N_{12}Na_2O_{30}$ $[M+2Na]^{2+}$ 1073.5422, found 1073.5496; CHN Analysis calc. for $C_{108}H_{156}N_{12}O_{30}$: C, 61.70; H, 7.48; N, 7.99; found: C, 59.57; H, 7.34; N, 7,74.

Synthesis of scrambled porous cages. The scrambled cage mixture was synthesized in one step via the reaction of 1,3,5-triformylbenzene (4 equiv.), 1,2-diamino-2-methylpropane[23] (3 equiv.), and (*R,R*)-1,2-diaminocyclohexane[6] (3 equiv.) in dichloromethane at room temperature (yield = 77 %). Full details are given in the Supplementary Information

Preparation the porous liquids. The crown-cage (0.100 g, 0.0475 mmol, 1 equiv.) was dissolved in 15-crown-5 (113 μL, 0.5707 mmol, 12 equiv.) by sonicating the mixture for 2 h, resulting in a viscous, pale yellow liquid. For the scrambled cages, the solid material was first degassed and then dissolved in rigorously purified hexachloropropene (PCP) to form a pale yellow 20 % w/v solution.

Molecular dynamics (MD) simulations. Atomistic models for the crown-cage were constructed using the OPLS all atom force-field[27]. We computed the free energy cost for introducing a single 15-crown-5 molecule into a cage cavity using the Umbrella Sampling (US) method[28] combined with the Weighted Histogram Analysis Method (WHAM)[29]. The US simulations were performed with the GROMACS-4.5.3 code[30], in the canonical ensemble (NVT) at 400 K, using a time-step of 0.001 ps. Bulk MD simulations were run on a sample comprising 40 cages and 480 solvent molecules enclosed in a cubic and periodic simulation box in the isobaric-isothermal ensemble (NPT), using a time-step of 1 fs, a Nose-Hoover thermostat[31,32], and a Parrinello-Rahman barostat[33], with time constants of 0.1 ps and 1 ps, respectively. Lennard-Jones interactions were cut off at 1.4 nm, while Coulomb forces were computed using the smooth particle mesh Ewald technique[34]. Full computational details are given in the Supplementary Information.

Positron annihilation lifetime spectroscopy (PALS). Measurements were performed as function of temperature in a standard experimental set up, as described previously[35].

Gas solubility measurements. An isochoric technique[36] was used to measure methane gas solubility in the pure 15-crown-5 solvent and in the porous liquid. For the scrambled cages, gas solubilities were either measured by ^{1}H NMR (*e.g.*, for methane) or, for larger bulk samples of the porous liquid, by displacing the gas by addition of an excess of a second, small guest (*e.g.*, chloroform, Fig. 5b) and measuring the amount of gas (*e.g.*, xenon) evolved.

Viscosity measurements. These were carried out using a calibrated RheoSense μVISC viscometer (0.01–100 cP) with a temperature controller (291–323 K). Measurements were repeated a minimum of three times.

Acknowledgements This work was funded by the Leverhulme Trust (F/00 203/T) and by EPSRC (EP/C511794/1). MGDP acknowledges financial support from ANPCyT (PICT-2011-2128). AIC acknowledges the European Research Council under the European Union's Seventh Framework Programme/ERC Grant Agreement no. [321156] for financial support. We thank M. E. Briggs for assistance with the cage syntheses. This project has received funding from the European Union's Horizon 2020 research and innovation programme under grant agreement No. 643998.

Author Contributions N.G. and R.L.G. synthesized the porous crown cage. M.D.P. and G.M. carried out the molecular simulations. K.R. and T.K. performed the PALS measurements. M.C.G. and L.P. measured the methane gas solubilities for the crown cage porous liquid. R.G. and A.I.C. conceived the synthesis of the scrambled porous imine cages. R.L.G synthesized and characterized the scrambled porous imine cage and measured the gas solubilities. S.L.J. led the project overall and conceived the non-interpenetrating crown-ether cage design. A.I.C. and S.L.J. led the writing of the manuscript with contributions from all coauthors.

1. Wright, P. A. Microporous framework solids (Royal Society of Chemistry, Cambridge, 2007).

2. Cheetham, A. K., Férey, G. & Loiseau, T. Open-framework inorganic materials, *Angew. Chem. Int. Ed.* **38**, 3268 (1999).

3. Kitagawa, S., Kitaura, R. & Noro, S. Functional porous coordination polymers, *Angew. Chem. Int. Ed.* **43**, 2334 (2004).

4. D'Alessandro, D. M., Smit, B. & Long, J. R. Carbon dioxide capture: Prospects for new materials. *Angew. Chem. Int. Ed.* **49**, 6058 (2010).

5. O'Reilly, N., Giri, N. & James, S.L. Porous liquids, *Chem. Eur. J.* **13**, 3020 (2007).

6. T. Tozawa, *et al.*, Porous organic cages, *Nature Mater.*, **8**, 973 (2009).

7. Jones, J. T. A. *et al.* Modular and predictable assembly of porous organic molecular crystals. *Nature* **474**, 367-371 (2011).

8. Robbins, T. A., Knobler, C. B., Bellew, D. R. & Cram, D. J. A highly adaptive and strongly binding hemicarcerand, *J. Am. Chem. Soc.* **116**, 111 (1994).

9. Chaffee, K. E., Fogarty, H. A., Brotin, T., Goodson, B. M. & Dutasta, J.-P., Encapsulation of small gas molecules by cryptophane-111 in organic solution. 1. Size and shape-selective complexation of simple hydrocarbons*, J. Phys. Chem. A.* **113**, 13675 (2009).

10. Little, M. A., Donkin, J., Fisher, J., Halcrow, M. A., Loder, J. & Hardie, M. J. Synthesis and methane-binding properties of disulfide-linked cryptophane-0.0.0*, Angew. Chem. Int. Ed.* **51**, 764 (2012).

11. Pohorille, A. & Pratt, L. R. Cavities in molecular liquids and the theory of hydrophobic solubilities, *J. Am. Chem. Soc.* **112,** 5066 (1990).

12. Pierotti, R. A. The solubility of gases in liquids, *J. Phys. Chem*., **67**, 1840 (1963).

13. Pierotti, R. A. A scaled particle theory of aqueous and non-aqueous solutions, *Chem. Rev.* **76**, 717 (1976).

14. Giri, N., *et al*., Alkylated organic cages: from porous crystals to neat liquids, *Chem. Sci.,* **3**, 2153 (2012).

15. Melaugh, G., Giri, N., Davidson, C. E., James, S. L. & Del Popolo, M. G. Designing and understanding permanent microporosity in liquids, *Phys. Chem. Chem. Phys.* **16**, 9422 (2014).

16. Mogensen, O. E. Ed., Positron annihilation in chemistry, Springer Series in Chemical Physics 58 (Springer, Berlin, 1995).

17. Mahmood, T., Cheng, K. L. & Yean, Y. C. Microanalysis of open spaces in crown ethers by using a novel probe: Positron annihilation spectroscopy, *Third International Workshop on Positron and Positronium Chemistry*, 640 (1990).

18. Lannung, A. & Gjaldbaek, J. C. The solubility of methane in hydrocarbons, alcohols, water and other solvents, *Acta Chim. Scand.* **14**, 1124 (1960).

19. Darwish, N. A., Gasem, K. A. M. & Robinson Jr, R. L. Solubility of methane in benzene, naphthalene, phenanthrene and pyrene at temperatures from 323 to 433 K and pressures to 11.3 MPa, *J. Chem. Eng. Data* **39**, 781 (1994).

20. Zhang, J. Chai, S.-H., Qiao, Z.-A., Mahurin, S. M., Chen, J., Fang,, Y., Wan, S., Nelson, K., Zhang, P., Dai, S. Porous liquids: A promising class of media for gas separation. *Angew. Chem., Int. Ed.* **54**, 932, (2015).

21. Houndonougbo, Y., Signer, C., He, N., Morris, W., Furukawa, H., Ray, K. G., Olmsted, D. L., Asta, M., Laird, B. B., Yaghi, O. M. A combined experimental-computational

investigation of methane adsorption and selectivity in a series of isoreticular zeolitic imidazolate frameworks. *J. Phys. Chem. C* **117**, 10326 (2013).

22. Jiang, S., Jones, J. T. A., Hasell, T., Blythe, C. E., Adams, D. J., Trewin, A., Cooper, A. I. Porous organic molecular solids by dynamic covalent scrambling. *Nat. Commun.* **2**, 207 (2011).

23. Hasell, T., Culshaw, J. L., Chong, S. Y., Schmidtmann, M., Little, M. A., Jelfs, K. E., Pyzer-Knapp, E. O., Shepherd, H., Adams, D. J., Day, G. M., Cooper, A. I. Controlling the crystallization of porous organic cages: Molecular analogs of isoreticular frameworks using shape-specific directing solvents. *J. Am. Chem. Soc.* **136**, 1438 (2014).

24. Chen, L. *et al.* Separation of rare gases and chiral molecules by selective binding in porous organic cages. *Nat. Mater.* **13**, 954 (2014).

25. Little, M.A., Donkin, J., Fisher, J., Halcrow, M. A., Loder, J., Hardie, M. J. , Synthesis and methane-binding properties of disulfide-linked cryptophane-0.0.0. *Angew. Chem., Int. Ed.*, **51**, 764 (2012).

26. Chaffee, K.E., Fogarty, H. A., Brotin, T., Goodson, B. M., Dutasta, J.-P., Encapsulation of Small Gas Molecules by Cryptophane-111 in Organic Solution. 1. Size and Shape-Selective Complexation of Simple Hydrocarbons. *J. Phys. Chem. A*, **113,** 13675 (2009).

27. Jorgensen, W. L., Maxwell, D. S. & Tirado-Rives, J. Development and testing of the OPLS all-atom force field on conformational energetics and properties of organic liquids, *J. Am. Chem. Soc.* **118**, 11225 (1996).

28. Roux, B. The calculation of the potential of mean force using computer-simulations, *Comput. Phys. Commun.* **91**, 275 (1995).

29. Kumar, S., Rosenberg, J. M., Bouzida, D., Swendsen, R. H. & Kollman, P. A. Multidimensional free-energy calculations using the weighted histogram analysis method, *J. Comput. Chem.* **13**, 1011 (1992).

30. Hess, B., Kutzner, C., van der Spoel, D. & Lindahl, E. GROMACS 4: Algorithms for highly efficient, load-balanced, and scalable molecular simulation, *J. Chem. Theory Comput*., **4**, 435 (2008).

31. Nose, S. A molecular-dynamics methods for simulations in the canonical ensemble, *Mol*. *Phys*. **52**, 255 (1984).

32. Hoover, W. G. Canonical dynamics - equilibrium phase-space distributions, *Phys. Rev. A: At., Mol., Opt. Phys*., **31**, 1695 (1985).

33. Parrinello, M. & Rahman, A. Polymorphic transitions in single-crystals - a new molecular-dynamics method, *J. Appl. Phys.,* **52**, 7182 (1981).

34. Essmann, U., Perera, L., Berkowitz, M. L., Darden, T., Lee, H. & Pedersen, L. G. A smooth particle mesh Ewald method, *J. Chem. Phys.* **103**, 8577 (1995).

35. Harms, S., Rätzke, K., Faupel, F., Schneider, G. J., Willner, L. & Richter, D. Free volume of interphases in model nanocomposites studied by positron annihilation lifetime spectroscopy, *Macromolecules* **43**, 10505 (2010).

36. Jacquemin, J. Costa Gomes, M. F., Husson, P. & Majer, V. Solubility of carbon dioxide, ethane, methane, oxygen, nitrogen, hydrogen, argon, and carbon monoxide in 1-butyl-3-methylimidazolium tetrafluoroborate between temperatures 283 K and 343 K and at pressures close to atmospheric, *J. Chem. Thermodynamics* **38**, 490 (2006).